

# Modeling of Shaped Beam Satellite Antenna Patterns

K. SUDHAKAR RAO, MEMBER, IEEE, AND HARRY J. MOODY

**Abstract**—A simple model for specifying the radiation characteristics of satellite antennas for use in orbit planning of the fixed satellite service (FSS) is developed. A new parametric template is derived for specifying the main beam and sidelobe radiation envelope of shaped beam antennas. The template is primarily described in terms of local component beamwidth/antenna size and the peak sidelobe level. The coverage region width in the direction of interest is used as a secondary parameter in deriving the parametric template. The new template is found to be reasonable based on the comparisons made with measured shaped beam patterns on current satellites.

## I. INTRODUCTION

AN IDEAL SATELLITE communications antenna would have uniform gain in the service area and no radiation beyond the coverage region. This, in principle, requires infinite antenna size and a large number of component beams. However, the sidelobe radiation outside the coverage area in practical situations is limited by the antenna size, amplitude, and phase illumination and excitation errors, the degree of frequency reuse provided, off-focus locations of some of the feeds combined with location errors, surface errors of the radiator, etc.

A variety of sidelobe templates have been proposed in the past in order to estimate the radiation sidelobes of satellite antennas for use in interference studies [1], [2]. Most significant among them are the broadcast satellite service (BSS) patterns and the International Radio Consultative Committee (CCIR) definitions. These templates are reviewed in [1] with relevant equations describing their characteristics. The BSS 1977 (WARC 1977) pattern is simply described in terms of the half-power (3 dB) beamwidth in the direction of interest. The roll-off characteristics beyond the coverage edge have been improved in the BSS 1983 fast roll-off patterns in which the template is described in terms of the elementary beamlet size and the 3 dB coverage width in a specified direction. The fixed satellite service (FSS) reference pattern (CCIR Report 558-2) assumes modest sidelobe levels of  $-20$  dB and is less stringent than the WARC 1977 patterns. Rice *et al.* [3] have proposed ideal antenna patterns that are applicable only to pencil beams.

A cosine envelope, instead of a Gaussian curve, was proposed in a recent CCIR study [2] to describe the main lobe

skirt region from the half-power point to the first null location. The advantage of this pattern is that the gain can be represented as a function of the peak sidelobe level. However, the cosine envelope represents a very stringent pattern which might be difficult to meet even for future satellite systems. Further, the cosine pattern is expressed in terms of peak sidelobe level and the beamlet size. The coverage region width is not taken into account in the formulation. Antenna radiation in all the above templates is modeled in both the main beam fall-off region outside the coverage area and the sidelobe region where potential interference exists. However, these templates have not been compared with the extensive measured satellite antenna data available in order to validate their use. Also, a reference envelope pattern for shaped beam antennas has not yet been formally defined by the CCIR.

A novel parametric template is derived in this paper, in terms of the beamlet size, peak sidelobe level, and the coverage region width, for describing the shaped beam characteristics of satellite antennas. Unambiguous representation of shaped beam patterns and proper utilization of the template are described. The new parametric template is more stringent than the existing reference patterns with the exception of the cosine curve [2]. It is found to be a reasonable upper bound specification for future satellite antennas based on the comparisons made with actual measurements on various satellite antennas. The new model, when compared to the previous ones, is a better representation of achievable antenna patterns and is also flexible enough to be used for preliminary interference investigations of future satellites that must operate in an interference limited environment.

## II. REPRESENTATION OF SHAPED BEAM ANTENNA PATTERNS

Pencil beam patterns for moderately scanned beams are characterized by the peak gain and the 3 dB beamwidth. Shaped beam patterns, however, do not conform to this model. Apart from the 3 dB beamwidth and the peak gain, the shaped beam antenna pattern depends on the coverage area on earth and also on the direction of measurement of the angular distance. Shaped beam patterns also depend on the extent of beam scan. Beam scanning effects are not particularly considered here with the intent of developing a simpler model for the radiation templates. However, the beam scan effects could be included in the templates to some degree by considering the 3 dB beamwidth of the component beam with scan.

The coverage contour of a shaped beam can be described by a minimum area ellipse circumscribing the actual area. The reference direction when using the templates was suggested in

Manuscript received September 19, 1985; revised March 1986. This work was supported by the Canadian Department of Communications under Contract 12ST-36100-4-4070 with the Department of Supply and Services.

The authors are with the Satellite and Aerospace Systems Division, Spar Aerospace Limited, 21025 Trans-Canada Highway, Ste-Anne-de-Bellevue, Quebec H9X 3R2, Canada.

IEEE Log Number 8714662.

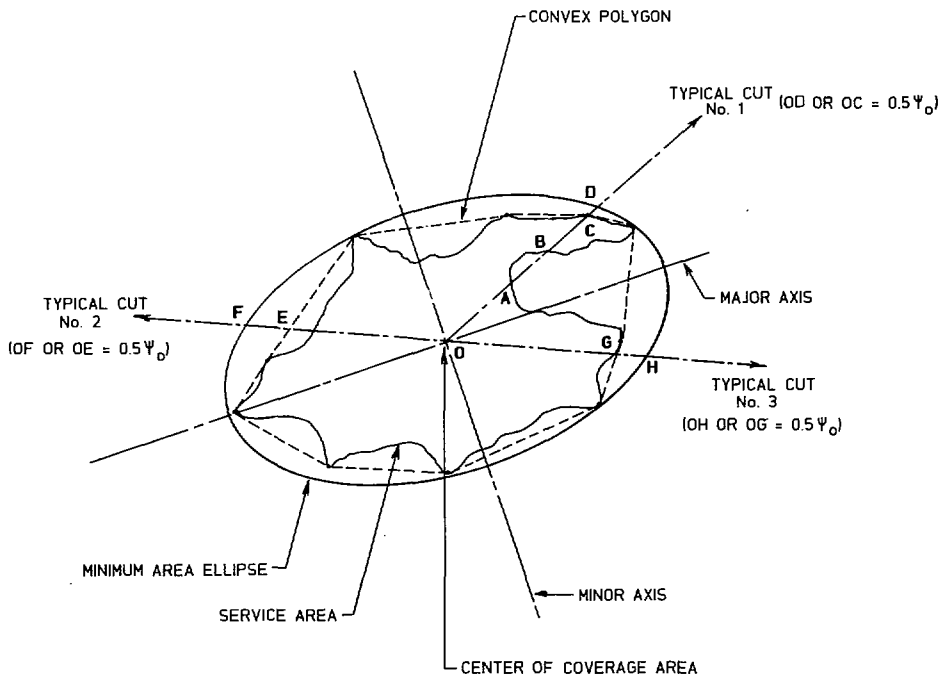


Fig. 1. Representation of shaped beam coverage region.

earlier studies to be orthogonal to the coverage area or to the constant gain contour. For concave portions of the gain contour, orthogonal direction of reference may intersect the coverage area more than once giving an ambiguous definition for the coverage area width. To circumvent this problem, the coverage area can be circumscribed by a contour which has no concavity. The reference pattern suggested in [2] is not an adequate representation of complex shaped beam patterns.

Unambiguous representation of the shaped beam antenna patterns is described as follows. The first parameter describing the reference pattern is the geographic coverage area. The center of the coverage area is traditionally defined as the intersection of the major and minor axes of the minimum area ellipse, circumscribing the coverage area. For a given coverage area, there exists a unique minimum area ellipse and hence the center of coverage is unambiguously defined [4], [5]. Different antenna pattern cuts should be straight lines passing through the center of the coverage area. The center of coverage area does not necessarily represent the beam center and is used only to define the axis of the pattern cuts. For certain coverage shapes, it might be appropriate to define the center of coverage area as the center of gravity of a convex polygon circumscribing the coverage region.

Another parameter describing the antenna patterns is the peak gain. Shaped beam patterns, however, may not have a unique peak gain point in the traditional sense. Instead, minimum coverage area gain (MCAG) can be used as a parameter. The MCAG is defined as the minimum gain occurring anywhere within the prescribed coverage area. The equivalent peak gain can then be defined by adding 3 dB to MCAG. In reality, the peak gain may be higher or lower than the equivalent peak gain value. The MCAG for shaped beams varies from 2 to 4.5 dB below the peak gain. It depends on the extent of beam shaping and frequency bandwidth. For area

coverage with high density beams such as the direct broadcast satellite (DBS) the MCAG is typically 2–2.5 dB below peak and for systems with low density beams (fewer beamlets) it is generally 4–4.5 dB below the peak gain. However, most of shaped beam satellites (Anik C, Brazilsat with primary coverage only, TDRSS etc.) operate with coverage gain approximately 3 dB below the peak gain.

The coverage area width ( $\psi_0$ ) is a parameter defining the shaped beam patterns. For a given pattern cut,  $\psi_0$  is defined as twice the angle between the coverage area edge in the direction of interest and the center of the coverage area as seen from the satellite. For coverage areas having concavity, it is suggested to use a convex polygonal representation of the coverage area, as shown in Fig. 1, and define  $\psi_0$  as twice the angular distance from the coverage center to the point of intersection on the polygon in a specified direction.

However, in directions having no concavity, the edge of coverage could be used for defining  $\psi_0$ . In cases where the contour gain synthesized pattern is available, the minimum gain contour of the coverage areas can be used to describe  $\psi_0$ .

The elementary beamwidth ( $\theta_0$ ) is the primary parameter which defines the shaped beam patterns. It is defined as the 3 dB beamwidth of the component beam closest to the coverage area in the specified direction. The width of the elemental beam with scan, if available, should be used as  $\theta_0$ . If the elementary beamlet size is unknown, the reflector size should be used as a parameter. For a -30 dB sidelobe level, the reflector size related to  $\theta_0$  is (from Table I)

$$\theta_0 \approx 79.62(\lambda/D)^0.$$

The derivation of templates in the main beam fall-off region of

<sup>1</sup> The chosen representation of the coverage area, whether it be an ellipse, polygon or synthesized contour, should include the antenna pointing error.

TABLE I  
PARAMETERS OF THE NEW TEMPLATE WITH PEAK SIDELobe LEVEL AS VARIABLE

$S_L$ (dB)	$\theta_o$ (degrees)	$\Delta\theta_L$ (degrees)	A	B	U	V	W	Z
-20	64.12 $\lambda/D$	54.74 $\lambda/D$	0.9276	0.618	0.326	2.684	0.854	1.966
-25	71.87 $\lambda/D$	67.49 $\lambda/D$	1.002	0.6952	-0.009	3.02	0.939	1.924
-30	79.62 $\lambda/D$	80.24 $\lambda/D$	1.077	0.7676	-0.324	3.335	1.008	1.891
-35	87.37 $\lambda/D$	92.99 $\lambda/D$	1.156	0.8381	-0.63	3.64	1.064	1.863
-40	95.12 $\lambda/D$	105.74 $\lambda/D$	1.2386	0.9071	-0.929	3.939	1.112	1.840

shaped beam antennas is shown in Section III with peak sidelobe level as variable. This enables one to compare the template with various measured data on current satellites having different sidelobe levels. The shaped beam templates are finally derived in Section IV by including all the parameters described above in the pattern definition.

### III. DERIVATION OF THE SHAPED BEAM TEMPLATE

Relevant analytical details and approximations made in deriving the shaped beam antenna template are described in this section. The template is initially expressed as a function of the sidelobe level and the elemental beamlet size. This gives flexibility to compare the template with measurements on current satellites, where the sidelobe radiation is less stringent. A new template for future satellites (assumed to have better sidelobe discrimination) is given later in Section IV using the analysis given here. The new template for shaped beam antennas will appropriately be referred to as a parametric template.

#### A. Analysis

Consider the amplitude illumination function of a circular aperture as

$$f(x) = \cos^N(\pi X/2) \quad (1)$$

in the region  $|X| \leq 1$ , where  $X$  is the distance from the center of the aperture being normalized to the aperture radius  $a$  ( $= D/2$ ). The secondary pattern due to  $f(X)$  for odd values of  $N$  is [6]

$$\frac{N! \cos u}{\prod_{K=0}^{(N-1)/2} [(2K+1)^2 - 4u^2/\pi^2]} \cdot \frac{2D}{\pi} \quad (2)$$

where  $D$  is the aperture diameter and  $u = (\pi D/\lambda) \sin \theta$ . In order to derive the approximate relationships between various antenna parameters, the following two cases are considered.

1) *Case A* ( $N = 1$ ): With  $N = 1$  in (2) the different antenna parameters of the secondary pattern are

$$S_L = -23 \text{ dB}, \theta_b = 34.38(\lambda/D), \theta_n = 85.94(\lambda/D), \\ \theta_s = 107.6(\lambda/D) \text{ and } \theta_{s2} = 167.8(\lambda/D)$$

where  $S_L$  is the level of first sidelobe level relative to beam maximum,  $\theta_b$  is the 3 dB half-beamwidth,  $\theta_n$  is the angular location of the first null,  $\theta_s$  is the angular location of the first sidelobe peak,  $\theta_{s2}$  is the angular location of the second sidelobe peak (all the angles are expressed in degrees) and also

$$\Delta\theta_n = \theta_n - \theta_b = 51.56^\circ(\lambda/D)$$

and

$$\Delta\theta_s = \theta_s - \theta_b = 73.22^\circ(\lambda/D).$$

2) *Case B* ( $N = 3$ ): The parameters of the secondary pattern for this case are  $S_L = -40 \text{ dB}$ ,  $\theta_b = 47.56^\circ(\lambda/D)$ ,  $\theta_n = 143.24^\circ(\lambda/D)$ ,  $\theta_s = 163.23^\circ(\lambda/D)$ ,  $\theta_{s2} = 222.5^\circ(\lambda/D)$ ,  $\Delta\theta_n = 95.68^\circ(\lambda/D)$  and  $\Delta\theta_s = 115.67^\circ(\lambda/D)$ .

The results of the above two cases are interpolated to express the angular parameters in terms of the peak sidelobe level and the aperture dimension ( $D/\lambda$ ) as

$$\theta_b = (16.56 - 0.775 S_L)^\circ(\lambda/D) \quad (3)$$

$$\Delta\theta_n = (-8.24 - 2.60 S_L)^\circ(\lambda/D) \quad (4)$$

$$\Delta\theta_s = (15.71 - 2.5 S_L)^\circ(\lambda/D) \quad (5)$$

and

$$\theta_{s2} = (93.74 - 3.22 S_L)^\circ(\lambda/D). \quad (6)$$

The main lobe skirt of the gain function is fitted through a Gaussian curve

$$G(\theta) = A \exp[-B(\theta/\theta_b)^2]. \quad (7)$$

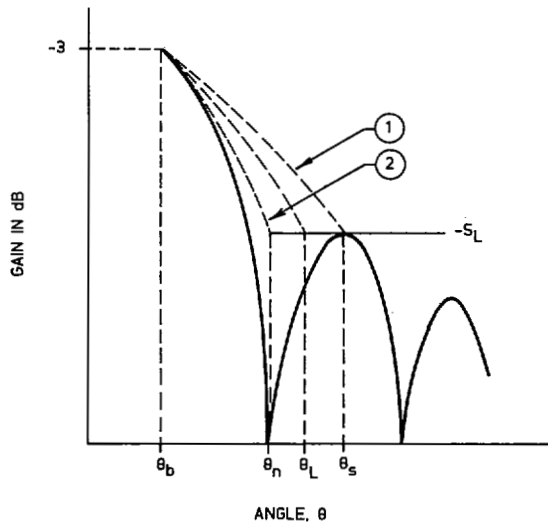


Fig. 2. Typical representations of main beam gain function beyond the edge of coverage of a shaped beam antenna.

The values of the constants  $A$  and  $B$  depend on the position of the truncation level of the sidelobe radiation. The truncation level  $S_L$  is initially assumed at the position of the first sidelobe peak and at the first null position. The constants  $A$  and  $B$  are determined using (3)–(5) and by using  $G(\theta_b) = 0.5$ . The main lobe skirt functions for the two cases are shown by curves 1 and 2 in Fig. 2 which correspond to truncation at the first sidelobe and first null locations, respectively. Extensive comparison of the two curves with measured results reveals that curve 1 is broader than the measurements and curve 2 represents optimistic values (especially close to the coverage region edge). A typical example of this fact is shown in Fig. 3, where measured results are taken in the North American zone of the TDRSS satellite antenna.

The truncation of the main lobe skirt function is hence taken at the mean angular location of the first null and the first sidelobe level. The resultant curve for the gain function  $G(\theta)$  falls between the two curves of Fig. 3 and represents an average of the two. The angular position of truncation of the gain function is given by

$$\Delta\theta_L = \theta_L - \theta_b = 1/2(\Delta\theta_n + \Delta\theta_s).$$

From (4) and (5)

$$\Delta\theta_L = (3.74 - 2.55S_L)^0(\lambda/D). \tag{8}$$

The constants  $A$  and  $B$  of the gain function depend on the peak sidelobe level and are obtained from the following:

$$0.5 = A \exp(-B) \tag{9}$$

$$10^{(S_L/10)} = A \exp \left[ -B \left\{ 1 + \frac{\Delta\theta_L}{\theta_b} \right\}^2 \right]. \tag{10}$$

The values of constants  $A$  and  $B$  for different peak sidelobe levels are shown in Table I. The variation of gain with the angle  $\Delta\theta$  is shown in Fig. 4 with the peak sidelobe level  $S_L$  as a parameter. For a given antenna dimension, the gain drop beyond the edge of coverage will be slower for improved

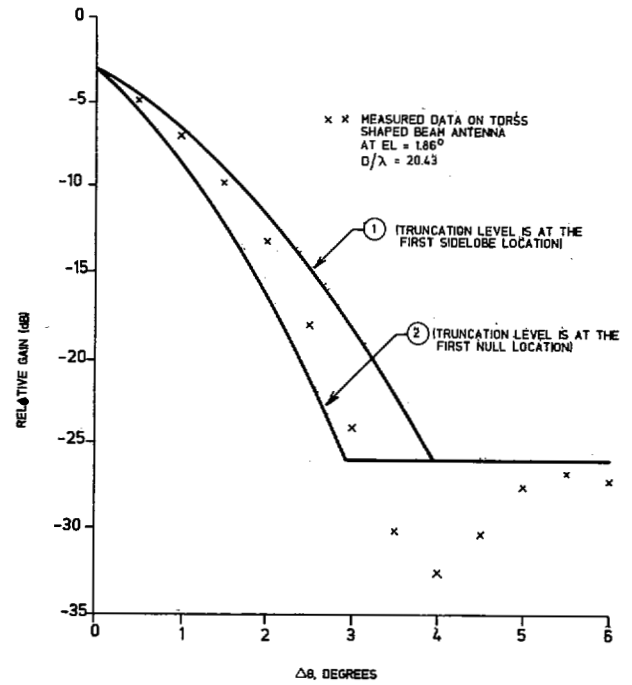


Fig. 3. Comparison of main beam co-polar gain curves with typical shaped beam measured gain data.

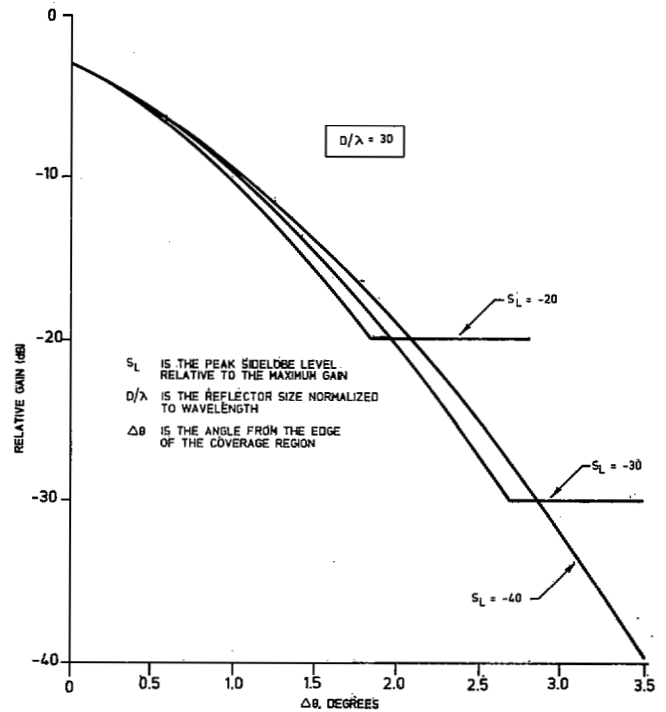


Fig. 4. Variation of gain with the angle (sidelobe level  $S_L$  is the parameter of the curves).

sidelobe levels. The aperture dimension is  $30 \lambda$  in the calculations of Fig. 4.

**B. Comparison of the Template with Shaped Beam Measured Data**

The templates derived in the previous section are compared here with available measured data from current satellites. The template curves are shown only in the main lobe region.

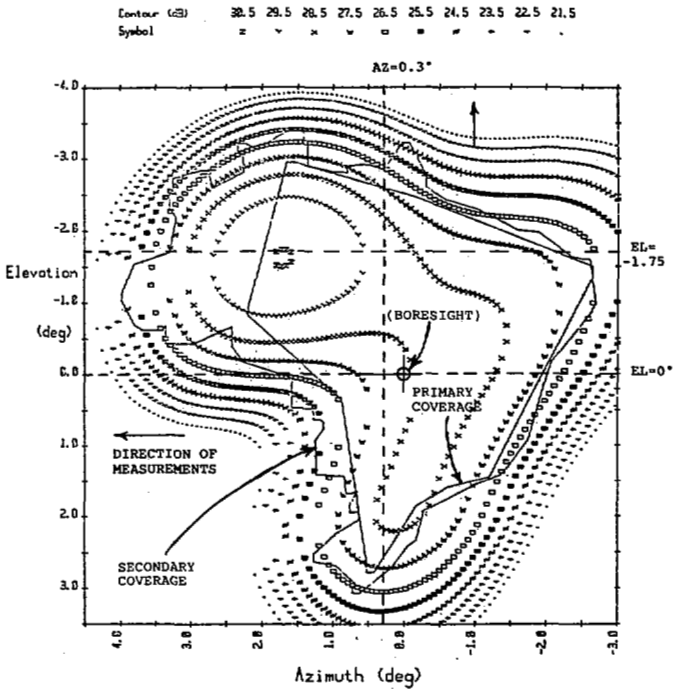


Fig. 5. Typical gain contour plot of Brazilsat shaped beam antenna (different pattern cuts and the direction of gain measurements are indicated).

However, the template is revised in Section IV in which the sidelobe region beyond the main lobe truncation angle is represented by proper curves.

The templates are initially compared with the measurements performed at Spar on a Brazilsat shaped beam antenna for the transmit case with horizontal polarization. The primary and secondary coverage gain requirements are 27 and 25 dBi. The primary area is the region bounded by the major cities of Brazil. The secondary area is that part of the country between the primary area and the geographical boundaries of Brazil. Gain contour plot at 3.96 GHz is shown in Fig. 5. It is obtained by synthesizing the scanned component beams and no sidelobe control is applied in the beam synthesis. The component beams are scanned approximately by the half-power beamwidth. The directions in which the measurements are taken are indicated by the arrows and the antenna boresight is shown in Fig. 5.

The following measured data are used for comparison with the templates:

- 1) elevation pattern at azimuth cut of  $0.3^\circ$
- 2) azimuth pattern at elevation cut of  $-1.75^\circ$
- 3) azimuth pattern at elevation cut of  $0^\circ$ .

The measured data for case 1) are shown in Fig. 6. The data are taken up to  $-11.23^\circ$  elevation to cover a few sidelobes. The measured results are compared with the templates in Fig. 6. The continuous line is the new template with  $S_L$  equals to  $-22$  dB and the dotted curve is the CCIR cosine envelope [2]. The CCIR cosine curve is too stringent and all the measurements fall above the curve. The measured values fall below the new template. The CCIR curve is too optimistic and the new curve is not too pessimistic when compared with the measurements. Brazilsat measured data for cases 2) and 3) are

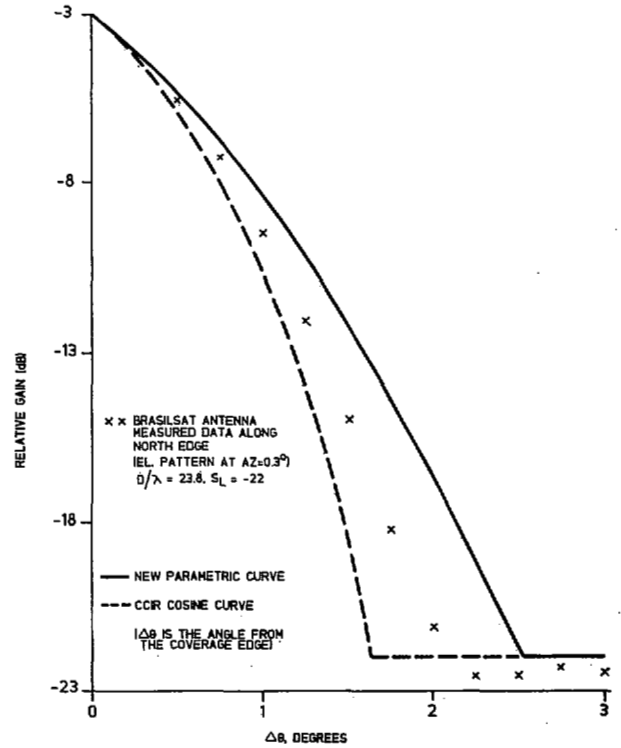


Fig. 6. Comparison of the parametric shaped beam template with Brazilsat measured data in the elevation plane (azimuth =  $0.3^\circ$ ).

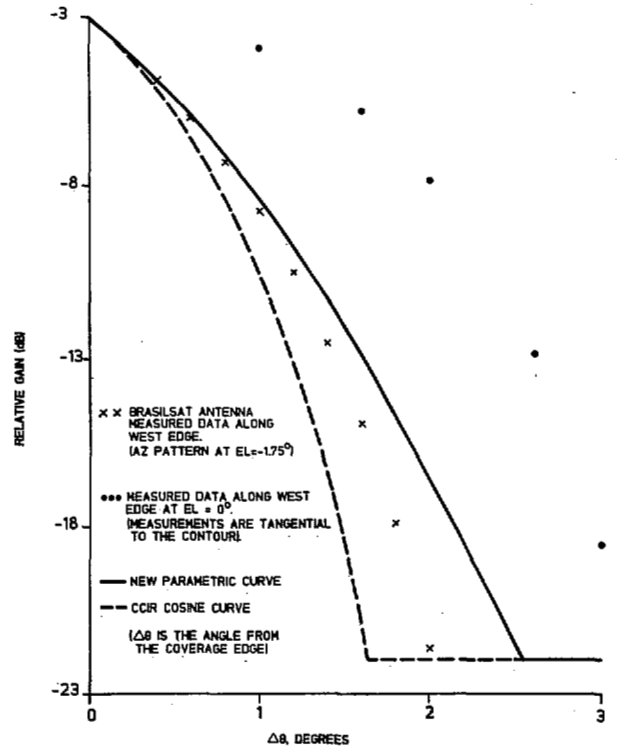


Fig. 7. Comparison of the parametric shaped beam template with Brazilsat measured data in the azimuth planes (elevation =  $1.75^\circ$  and  $0^\circ$ ).

shown in Fig. 7 along with the two template curves. Again, the CCIR curve shows optimistic isolation values and measured values in both elevation cuts fall above this template. The new template gives reasonable beam isolation values outside the coverage area for case 2). However, the measurements in  $0^\circ$

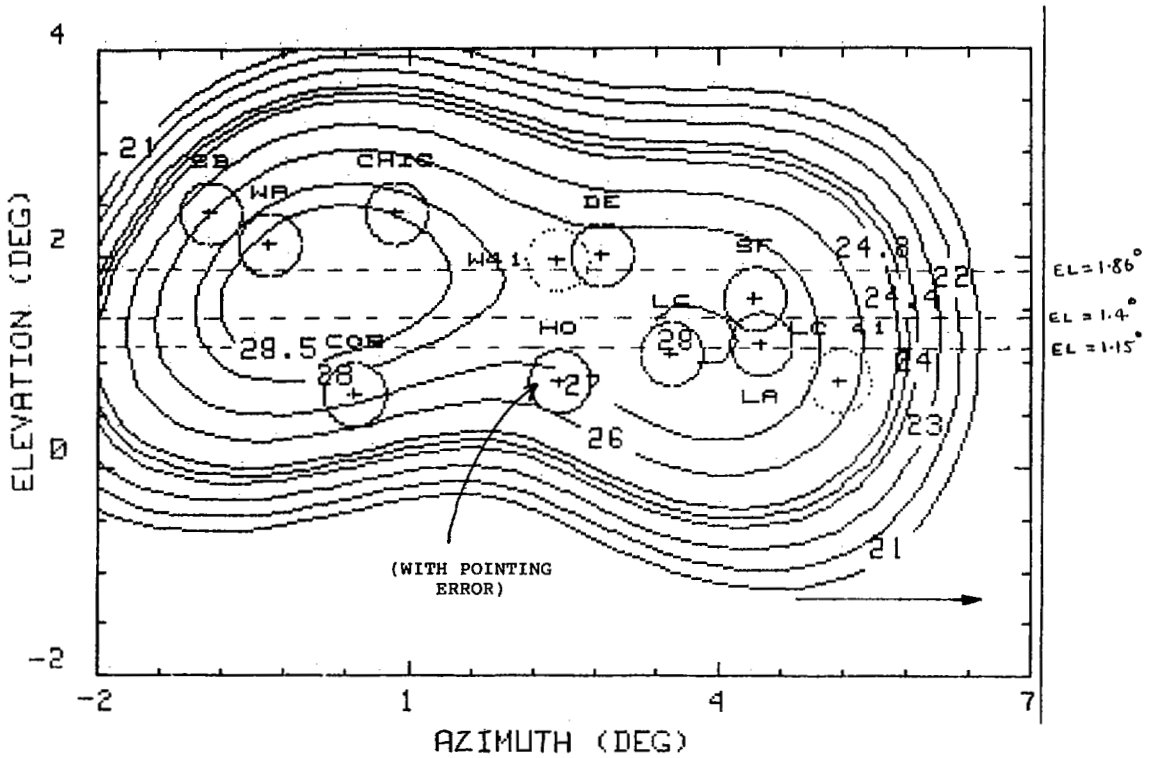


Fig. 8. Typical gain contour plot of TDRSS shaped beam.

elevation cut fall outside the new curve. This is due to the fact that measurements for case 3) are taken in a direction tangential to the coverage contour (See Fig. 5). The gain drop outside the coverage area, therefore, is less sharper than the parametric template. This shows that in directions where the coverage contour is tangential, the use of any template for beam isolation calculations is not advisable.

Measured data on TDRSS shaped beam antenna are used to compare the validity of the new templates. Fig. 8 shows the North American coverage gain contour plot of the TDRSS reflector antenna with  $D/\lambda = 20.43$ . The beam is synthesized by adding scanned component beams and no special means of controlling the sidelobe radiation outside the coverage area are employed in the beam synthesis. The antenna boresight is at Washington (marked WA in Fig. 8). Data measured in three constant-elevation planes of  $1.15^\circ$ ,  $1.4^\circ$ , and  $1.86^\circ$  are shown in Figs. 9-11. The CCIR envelope again proves to be optimistic and the new curve represents the measured values within reasonable limits. Fig. 12 shows the Intelsat V measured data for the hemispheric beam ( $8^\circ$  wide [2], measured in the western direction) along with the template curves. The new envelope curve matches fairly well with the measurements. The beam isolation values of the new curve close to the coverage edge are approximately 1 dB better than the measured values. The CCIR cosine curve again proves to be optimistic.

**C. Shaped Beam Pattern Roll-Off Characteristics**

The main beam roll-off characteristics of shaped beam antennas depend primarily on the reflector size and the degree of beam scan for a given frequency. The separation angle ( $\Delta\theta_L$ ) from the edge of a coverage region to the polar angle

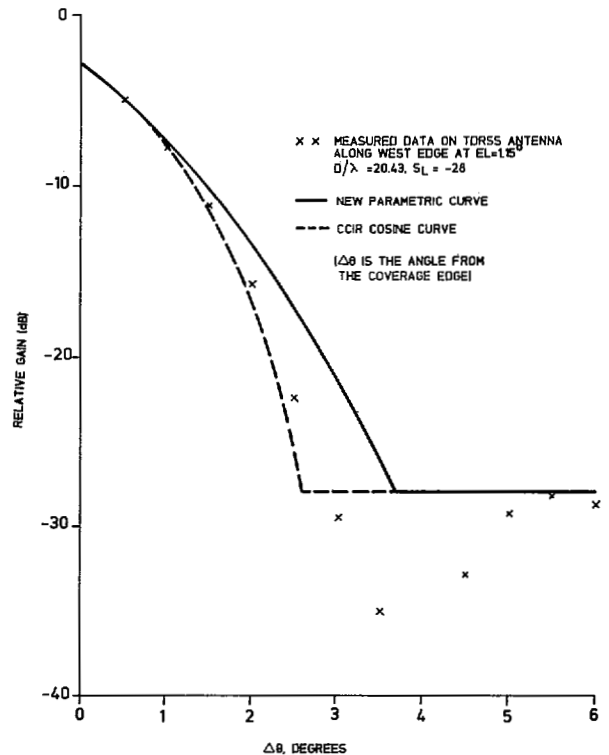


Fig. 9. Comparison of the parametric shaped beam template with TDRSS measured data in the azimuth plane of elevation =  $1.15^\circ$ .

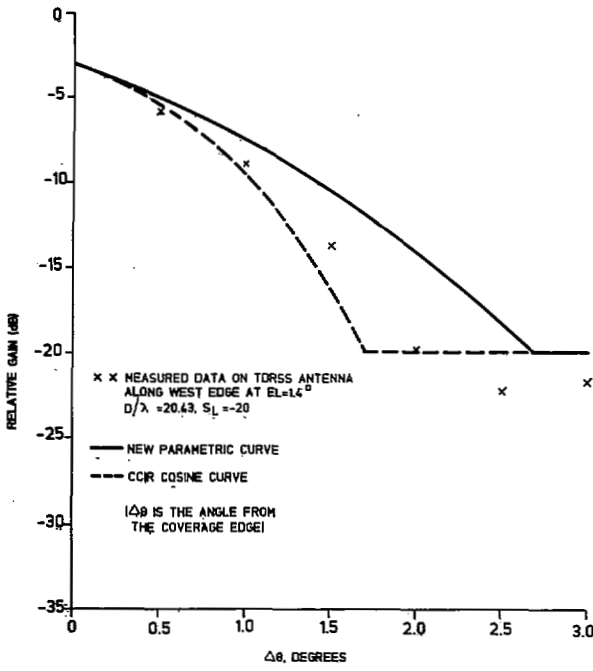


Fig. 10. Comparison of the parametric shaped beam template with TDRSS measured data in the azimuth plane of elevation = 1.4°.

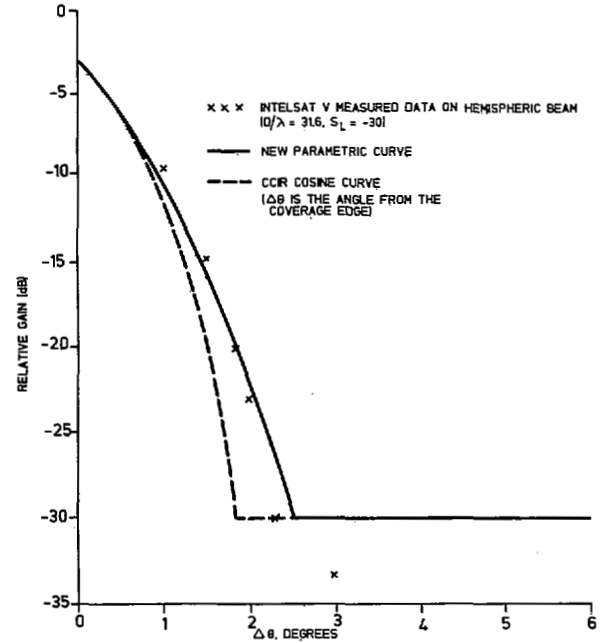


Fig. 12. Comparison of the parametric shaped beam template with Intelsat V measured data on hemispheric beam (beamwidth is 8° [2]).

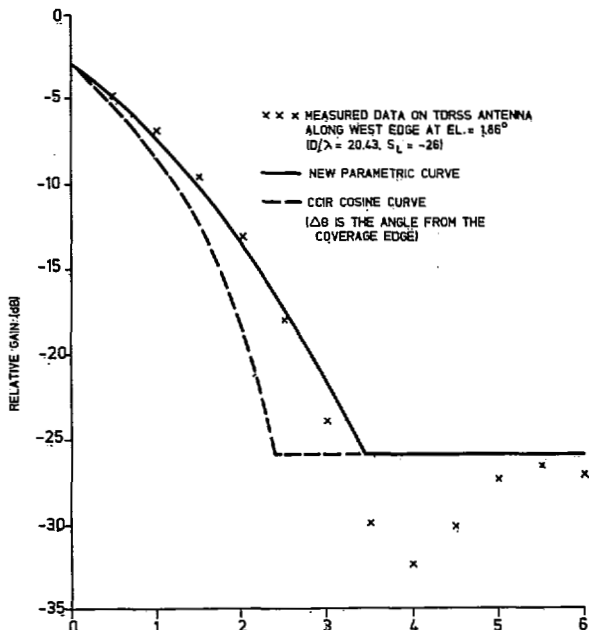


Fig. 11. Comparison of the parametric shaped beam template with TDRSS measured data in the azimuth plane of elevation = 1.86°.

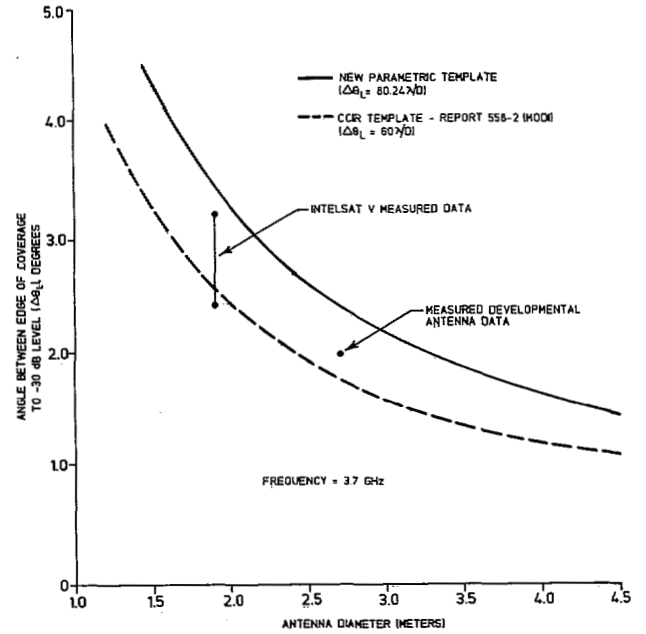


Fig. 13. Shaped beam antenna pattern roll-off characteristics with aperture size (frequency = 3.7 GHz). Measured data points correspond when emphasis is placed on achieving low sidelobes ([2, Annex IV]).

corresponding to -30 dB radiation level with respect to peak equivalent gain, from Table I, is given as

$$\Delta\theta_L = 80.24^\circ(\lambda/D). \tag{11}$$

The above relationship is plotted in Figs. 13 and 14 at 3.7 GHz and 11 GHz, respectively. Measured data is represented in these figures by discrete points and is obtained when sidelobe suppression technique is employed in the designs. The CCIR

cosine curve having a

$$\Delta\theta_L = 60^\circ(\lambda/D) \tag{12}$$

relationship is also shown by dotted lines.

The antenna dimensions according to the new template and the measured data points indicate that desired discrimination levels or better could be achieved in practice by using the template curves. The antenna size, as given by the CCIR cosine curve, seems to be optimistic when compared to the

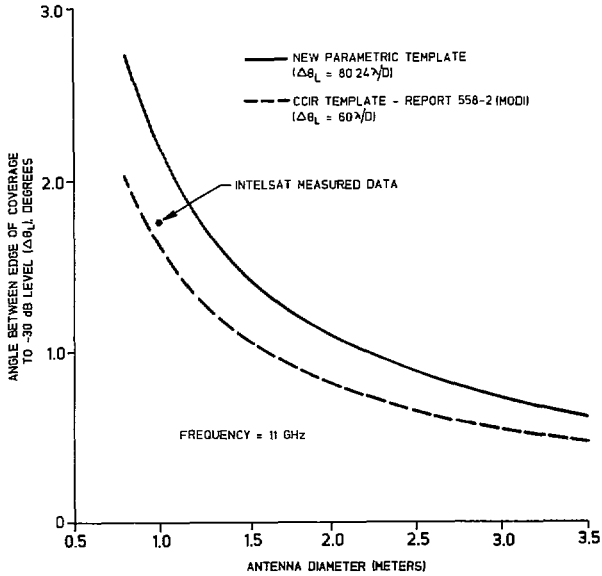


Fig. 14. Shaped beam antenna pattern roll-off characteristics with aperture size (frequency = 11 GHz). Measured data point corresponds when sidelobe suppression design technique is utilized [10].

actual size and required discrimination levels might be difficult to achieve. The new curve, therefore, when used for beam isolation calculations in orbit planning should give estimates that are closer to realistic values. It should be pointed out that the relationship given above ((11)) is only approximate and the actual relationship between  $\Delta\theta_L$  and  $(D/\lambda)$  depends on other secondary effects and is more complex.

#### IV. PARAMETRIC TEMPLATE FOR SHAPED BEAM SATELLITE ANTENNAS

##### A. Formulation

The new template is represented as a function of the peak sidelobe level in Section III. The main lobe skirt function beyond the edge of coverage is formulated as a Gaussian curve in the region  $\theta_b \leq \theta \leq \theta_b + \Delta\theta_L$ . Beyond the region  $\theta > \theta_L$ , the gain function is assumed constant at the first sidelobe level ( $S_L$ ) value. However, the sidelobe level decays with  $\theta$  in this region. Also, the envelope described in Section III is shown only as a function of  $\theta_b$  (or  $D/\lambda$ ) and the sidelobe level  $S_L$ . For a general case, the elementary beamlet size could be different from the coverage contour width. Hence, another parameter describing the coverage contour width in a specified direction has to be introduced to make the templates more general.

Let  $\psi_b = \psi_0/2$  represents the coverage region width from the center of the coverage area and  $\theta_b = \theta_0/2$  be the 3 dB half-width of the elementary beamlet. Fig. 15 shows a general representation of gain function. The edge of the coverage ( $\psi_b$ ) is assumed to be illuminated at 3 dB below the peak equivalent gain value (see Section II). Beyond the edge of coverage, the gain fall is dictated primarily by the elementary beamlet size (or the antenna size  $D/\lambda$ ) and the coverage region width will have a second order effect.<sup>2</sup> Replacing the variable  $\theta$  with  $\psi$

<sup>2</sup> The feed illumination taper effect is taken into account by expressing the gain as a function of the peak sidelobe level. Even though beam scan effects are not included in the analysis, they can be accounted for to a certain extent by using the 3 dB beamwidth of the elemental beam with scan instead of  $\theta_0$  in the template.

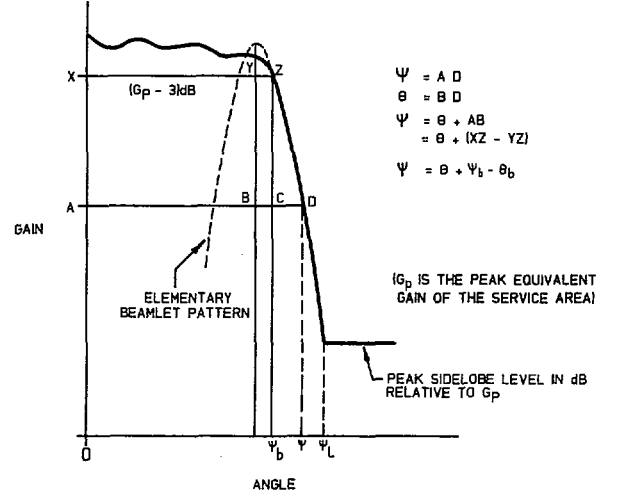


Fig. 15. Shaped beam pattern represented in terms of beamlet size and the coverage region width.

and using (see Fig. 15)

$$\psi = \theta + \psi_b - \theta_b \quad (13)$$

the gain function (given by (7)) becomes

$$G(\psi) = A \cdot \exp \left[ -B \left( \frac{\Psi_0}{0.5\theta_0} \right)^2 \cdot \left( \frac{\Psi - \Psi_b + \theta_b}{\Psi_0} \right)^2 \right]. \quad (14)$$

The above equation is valid in the region  $\psi_b \leq \psi \leq \psi_L$ , where

$$\psi_L = \theta_L + \psi_b - \theta_b = W \cdot \theta_0 + \psi_b \quad (15)$$

and

$$W = (3.74 - 2.55 S_L) / (33.12 - 1.55 S_L). \quad (16)$$

Expressing the gain function  $G(\psi)$  in decibels, (14) becomes

$$G_{dB} = G_p - \left[ U + V \left( \frac{\Psi_0}{0.5\theta_0} \right)^2 \left\{ \frac{\Psi}{\Psi_0} - 0.5 \left( 1 - \frac{\theta_0}{\Psi_0} \right) \right\}^2 \right]; \quad (17)$$

$$0.5 < \frac{\Psi}{\Psi_0} \leq 0.5 + W \left( \frac{\theta_0}{\Psi_0} \right).$$

The gain envelope is kept at a constant level corresponding to the peak sidelobe radiation in the region covering  $\psi_L$  and the position of the second sidelobe  $\psi_{s2}$ , which is given as

$$\Psi_{s2} = \Psi_0 \left[ Z \frac{\theta_0}{\Psi_0} + 0.5 \right] \quad (18)$$

where

$$Z = (77.18 - 2.445 S_L) / (33.12 - 1.55 S_L). \quad (19)$$

The gain curve in the constant sidelobe region is given as

$$G_{dB} = G_p - (-S_L);$$

$$0.5 + W \left( \frac{\theta_0}{\Psi_0} \right) < \frac{\Psi}{\Psi_0} \leq 0.5 + Z \left( \frac{\theta_0}{\Psi_0} \right). \quad (20)$$

The sidelobe fall-off region slope is taken as  $-20 \log(\psi/\psi_0)$  as used in the BSS 1983 fast roll-off patterns. The gain envelope in this region is given as

$$G_{dB} = G_p - \left[ -S_L - 20 \log \left( Z \frac{\theta_0}{\Psi_0} + 0.5 \right) + 20 \log (\Psi/\Psi_0) \right];$$

$$0.5 + Z \left( \frac{\theta_0}{\Psi_0} \right) < \frac{\Psi}{\Psi_0} \leq \frac{90}{\Psi_0}. \quad (21)$$

The upper bound of  $(\psi/\psi_0)$  in (21) can be taken as  $(90/\psi_0)$  with  $\psi_0$  expressed in degrees. Beyond this region the gain function is very much dependent on the spacecraft structure and the antenna location on the spacecraft. The new parametric template for satellite antennas is summarized as (the gain function  $G$  is in dB)

$$G = G_p - 12(\Psi/\Psi_0)^2; \quad 0 \leq (\Psi/\Psi_0) \leq 0.5, \quad (\text{coverage region}) \quad (22a)$$

$$G = G_p - \left[ U + V \left( \frac{\Psi_0}{0.5\theta_0} \right)^2 \left\{ \frac{\Psi}{\Psi_0} - 0.5 \left( 1 - \frac{\theta_0}{\Psi_0} \right) \right\}^2 \right];$$

$$0.5 < \frac{\Psi}{\Psi_0} \leq 0.5 + W \left( \frac{\theta_0}{\Psi_0} \right), \quad (\text{main lobe skirt region}) \quad (22b)$$

$$G = G_p - (-S_L); \quad 0.5 + W \left( \frac{\theta_0}{\Psi_0} \right) \leq \frac{\Psi}{\Psi_0} \leq 0.5 + Z \left( \frac{\theta_0}{\Psi_0} \right), \quad (\text{constant sidelobe region}) \quad (22c)$$

$$G = G_p - \left[ (-S_L) - 20 \log \left( Z \frac{\theta_0}{\Psi_0} + 0.5 \right) + 20 \log (\Psi/\Psi_0) \right];$$

$$0.5 + Z \left( \frac{\theta_0}{\Psi_0} \right) < \frac{\Psi}{\Psi_0} \leq \frac{90}{\Psi_0}, \quad (\text{sidelobe decay region}). \quad (22d)$$

$G_p$  in the above equations is the peak equivalent gain of the coverage area (see Section II) expressed in dB. The constants describing the new template with peak sidelobe level as parameter are given in Table I. For highly shaped beams having smaller  $\theta_0/\psi_0$  ratio, the upper limit of the constant sidelobe region (22c) moves closer to the coverage area. This aspect has not been considered in the reference patterns proposed in the past [1]-[4]. Also, the upper limit of (22c) becomes the second sidelobe peak location when  $\theta_0 = \psi_0$  (pencil beam case). For future satellites, peak sidelobe levels of  $-30$  dB could be achieved in a few directions (where potential interference with other service areas exists) by using special techniques such as use of nulling horns [5]. Other methods of reducing the sidelobe levels are described earlier [7]-[9]. The reference template for future satellites is described by (22) with  $S_L \approx -30$ .

### B. Comparison of the Parametric Template with the Measured Data

Fig. 16 compares the new parametric template with the measured performance of a developmental shaped beam antenna system with approximately  $40 \lambda$  aperture size [10]. This antenna represents the maximum C-band nonfurlable conventional reflector which can be accommodated by present-day launch vehicles. The BSS 1977 and the BSS 1983 reference patterns are also shown in Fig. 16. The parametric curve matches well with the measured pattern, whereas the BSS 1977 curve is far too broad with respect to the measurements. The 1983 BSS curve, however, agrees well with measured gain values only in the main beam fall-off region. It is a less stringent specification in the sidelobe region of the shaped beam gain measurements.

The three templates are compared with Intelsat V pre-launch measured data on eastern zonal beam in Fig. 17. The parametric curve represents the closest upper bound envelope of the measurements in the main beam fall-off region. However, the parametric curve seems stringent in the sidelobe region. This is due to the fact that the peak sidelobe level obtained in the measurements was around  $-25$  dB.

### C. Implication of the Template in Terms of Orbit-Utilization

The requirement for low sidelobes originates from the need for frequency reuse. In the case of satellite antennas, frequency reuse by means of spatial isolation occurs when the satellite has two or more antenna beams widely separated on the ground. Interference into one beam is caused by sidelobes of the other beam falling within the coverage area of the first beam. The antennas for the two beams may be on the same satellite or on two separate satellites in the same slot. An additional interference can occur from ground stations within the main beam but directed at another satellite as well as from ground stations not in the main beam area and directed at another satellite. Protection from the first of these is provided by the directivity of the ground antenna while the second is suppressed by the sidelobe performance of both ground antenna and the spacecraft antenna.

Although low sidelobes have not been a primary requirement for spacecraft antennas in the past, the requirement to maximize main beam gain has ensured that a level of about 20 dB below peak has generally been maintained. This has been true in spite of the complex nature of the antenna and variation in feed horn sizes and illumination function across the feed assembly.

In considering the beam template outside the main beam area, there are regions where the sidelobe level is immaterial as when the sidelobe misses the earth entirely, i.e., the northern sidelobes of the Canadian Anik-D satellite or when the sidelobe falls in an ocean region. There are also cases where the sidelobe misses the earth but is in the orbital plane so that it may illuminate other geostationary satellites. Since the downlink frequencies are not generally reused on the uplink, this is not generally an interference problem but may be in certain cases. Any requirements for sidelobe control apply only to those regions where interference is a potential problem

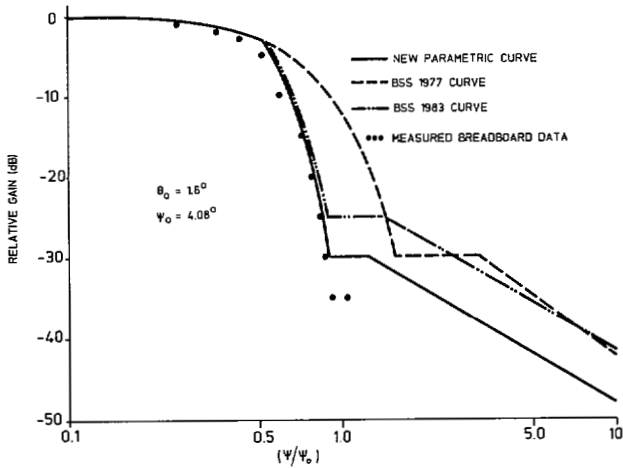


Fig. 16. Comparison of parametric shaped beam template with measured data on a developmental offset reflector antenna.

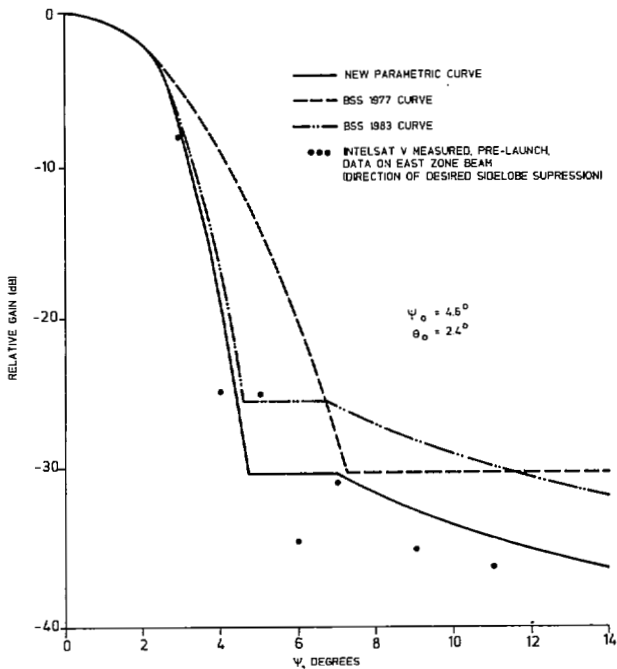


Fig. 17. Comparison of parametric shaped beam template with measured data on Intelsat V east-zone beam.

and not those regions where there is no possibility of interference. A major question in the application of the templates is how close two coverage areas can be, using the same frequency band from the same orbital slot. This is related to the beamwidth of the beamlet which is related to the size of the main reflector.

The closer the two areas are to each other, the larger the reflector must become. There is a practical limit to the size of the reflector determined by space and weight considerations. In addition, a minimum cost system will require a reflector size within a limited range. Thus, any plan for frequency reuse should not assign the same frequency from the orbital slot to closely adjacent areas. In this way, uneconomical space segment costs will not be imposed on the two areas. Regions closer than this, and specifically the region covered by the side

of the main beam cannot be used for frequency reuse and the template in this region should not impact the design of the antenna.

V. SUMMARY AND CONCLUSION

The development of a model for shaped beam antenna sidelobe radiation fall-off for future satellites is described in this paper for orbit planning purposes. A new template is derived in terms of shaped beam parameters and is compared with measurements on various satellite antennas. The implications of this template in terms of orbit utilization are discussed. The basic conclusions are given as follows.

1) Shaped beam parametric template can be modeled in terms of elementary beamlet size and the coverage area width. It is assumed that the radiation outside the coverage region depends basically on the beamlet size (or antenna size) and the coverage area width in the direction of interest is used as a secondary parameter to describe the template in an unambiguous fashion.

2) The new template derived is found to be reasonable based on the comparisons made with measured patterns on several current satellites.

3) Shaped beam patterns can be described by a minimum area ellipse, a polygon or a synthesized contour representation of the coverage area whichever is most appropriate in terms of the direction and the complexity of the coverage area. In any case, the coverage area representation should include the pointing error.

4) The use of shaped beam parametric template should be restricted to directions where there is potential radiation interference to other neighboring areas. Otherwise, the sidelobe suppression constraints may have a severe impact on the antenna size and complexity. A good example where a problem could arise is with a highly shaped beam where the pattern cut of interest runs parallel (or nearly parallel) to the contour. It is shown by an example in Section III (Fig. 7) that the antenna pattern envelope in this case exceeds the recommended sidelobe template. Thus, the application of sidelobe templates must be consistent with coverage regions where the beam is required to have a steep slope.

5) The new parametric template is more stringent than the BSS 1977 (WARC 1977) reference pattern in the main beam and sidelobe regions. The new template is close to the BSS 1983 fast roll-off pattern, though slightly more stringent in the main beam fall-off and sidelobe decay regions. Also, it is more stringent than RARC 1983 pattern and FSS pattern in the main beam and sidelobe regions. The CCIR cosine pattern is found to be more stringent than the parametric template and might be a difficult specification even for future satellites.

6) Future satellite antennas with sidelobe levels better than -30 dB might require larger aperture sizes (typically 20 percent more) and also more number of feed elements. Shaping techniques on single as well as dual reflectors and optimization techniques could be used for maximizing the coverage area gain and minimizing the radiation outside the coverage region. Also, techniques for reducing peak sidelobe levels in desired directions (with potential interference problem) and increasing the farout sidelobe envelope slope could

be adopted for future antennas in order to enhance orbit utilization.

7) All of the techniques for reducing the sidelobe levels have an impact on size and weight of the spacecraft antenna with accompanying increase in cost.

#### ACKNOWLEDGMENT

The authors would like to thank Mr. K. E. Brown and Mr. R. J. Bibby of the Department of Communications, Ottawa, Canada for many useful suggestions and encouragement. The authors are indebted to the anonymous reviewers for their critical review and useful suggestions which have helped in revising the paper.

#### REFERENCES

- [1] "Intelsat contribution to CCIR interim working party 4/1," Attachment no. 1 to BG-57-55E W/12/83, February 1984.
- [2] CCIR Report 558-2 (MOD I), "Satellite antenna patterns in the fixed-satellite service," Study Programme 2J/4, 1984.
- [3] P. L. Rice, W. T. Thompson, and J. L. Noble, "Idealized pencil beam antenna patterns for use in interference studies," *IEEE Trans. Commun. Technol.*, vol. COM-18, no. 1, pp. 27-32, Feb. 1970.
- [4] CCIR Study Group Document 4/253-E (1982-1986), "Spacecraft shaped beam antenna pattern," Revision to Rep. 558-2, June 1985.
- [5] K. S. Rao, "Development of a model for satellite antenna sidelobe characteristics for use in orbit planning in the fixed satellite service," Spar Aerospace Limited, Ste-Anne-de-Bellevue, Quebec, Canada, Report RML-009-85-05, Jan. 1985.
- [6] S. Silver, *Microwave Antenna Theory and Design*. U.K.: Peter Peregrinus Ltd., 1984, ch. 6.
- [7] R. L. Fante, P. R. Franchi, N. R. Kernweis and L. F. Denmet, "A

parabolic cylinder antenna with very low sidelobes," *IEEE Trans. Antennas Propagat.*, vol. AP-28, no. 1, pp. 53-59, Jan. 1980.

- [8] P. A. Venkatachalam, N. Gunasekaran, and P. Ramanujam, "A parabolic reflector with asymmetric low sidelobes," *IEEE Trans. Antennas Propagat.*, vol. AP-32, no. 8, pp. 873-876, Aug. 1984.
- [9] J. J. Lee and R. L. Carlise, "A coma-corrected multibeam shaped lens antenna, Part II: Experiments," *IEEE Trans. Antennas Propagat.*, vol. AP-31, no. 1, pp. 216-220, Jan. 1983.
- [10] P. Ackerman, private communication, Hughes Aircraft Co., Dec. 1984.

**K. Sudhakar Rao** (M'83), for a photograph and biography please see page 366 of the April 1987 issue of this TRANSACTIONS.



**Harry J. Moody** was born in Birsay, Saskatchewan, Canada, on May 8, 1926. He received the Bachelor of Engineering and Master of Science degrees from the University of Saskatchewan, Canada, in 1948 and 1950, respectively, and the Ph.D. degree from McGill University, Montreal, Canada, in 1955.

He has worked for the National Research Council in Ottawa. From 1956-1961 he was employed by the Canadian Marconi Company Research Laboratory in Montreal and worked on a number of projects. In 1961 he joined the RCA Research Laboratories in Montreal to work on millimeter wave studies, counter mortar radar antennas and millimeter wave propagation measurements. Later he became involved in satellite programs and contributed to most proposals and satellite studies. In 1977 RCA sold its Satellite and Communications business in Canada to Spar Aerospace Limited with a transfer of all employees. Since then he has continued his satellite activities with major involvement in the M-Sat design studies and the Anik E proposal.